
The Semi-Diurnal Tides along the Equator in the Indian Ocean

L. A. Fairbairn

Phil. Trans. R. Soc. Lond. A 1954 **247**, 191-212

doi: 10.1098/rsta.1954.0017

Email alerting service

Receive free email alerts when new articles cite this article - sign up in the box at the top right-hand corner of the article or click [here](#)

To subscribe to *Phil. Trans. R. Soc. Lond. A* go to: <http://rsta.royalsocietypublishing.org/subscriptions>

THE SEMI-DIURNAL TIDES ALONG THE EQUATOR IN THE INDIAN OCEAN

By L. A. FAIRBAIRN

Oceanography Department, University of Liverpool

(Communicated by J. Proudman, F.R.S.—Received 9 March 1954—Revised 8 June 1954)

CONTENTS

	PAGE		PAGE
1. Introduction	191	8. Tidal data	201
2. The tidal theorem	193	9. Interpolated values of the harmonic constants	202
3. Application of the tidal theorem	194	10. Corrections for the Andaman Basin	204
4. The use of auxiliary functions independent of longitude	196	11. Integration	206
5. The use of auxiliary functions containing a factor e^{imx}	197	12. The equatorial distribution of tidal constituent K_2	208
6. Mean depth of the Indian Ocean north of the equator	199	13. Discussion of the results	210
7. Computation of auxiliary functions for $\pm m, \pm 2m, \pm 3m$	199	References	212

The distribution of the semi-diurnal tidal constituent K_2 along the equator has been calculated with the aid of known harmonic constants at approximately fifty coastal stations in the northern part of the Indian Ocean. This has been achieved by use of a theorem in tidal dynamics, which connects integrals involving the tidal elevations and currents along the boundaries of an oceanic region and the equilibrium elevation over its surface. The distribution of K_2 along the equator has been obtained in the form of a Fourier cosine series.

The depth of the ocean has been taken as uniform, except where corrections have been applied to the tidal data in areas where the water is very shallow. In the equatorial distribution the variations of phase give supporting evidence for recent co-tidal charts of the ocean. In addition, however, an estimate for the amplitude of the constituent is given for any point on the equator. This is believed to be the first direct arithmetical calculation of oceanic tidal distribution.

1. INTRODUCTION

The measurement of tides in mid-ocean is a problem involving great practical difficulties which have yet to be overcome. At present only theoretical methods have been employed to find the tidal distribution over the oceans. These methods may be divided into two groups, those depending only on a knowledge of coastal tides and those based on dynamical principles.

Co-tidal charts, in which lines are drawn through all points with simultaneous high water, provide a most effective means of showing the phase distributions of the tides. The first

chart of this type giving the principal features of the semi-diurnal tides in the major oceans was produced by Whewell in 1833. This merely joined up points on the coasts which had the same times of high water. The only dynamical reasoning concerned the curvature of the co-tidal lines and this was subsequently shown to be incorrect.

Using the hypothesis that the main characteristics of the tides can be reproduced by subdividing the oceans into a number of areas each containing oscillations with period 12h 25 min, Harris (1904) constructed charts of co-tidal lines for all the oceans and seas. This work is largely qualitative, giving no absolute amplitudes and neglecting the dynamical effects of the earth's rotation.

In 1920 Sterneck published charts for the semi-diurnal tides of the oceans which were based on interpolation of observations. Incorporating all the tidal data at that time available, Dietrich produced in 1944 a series of charts for the semi-diurnal constituents M_2 and S_2 and also for the diurnal constituents K_1 and O_1 . More recently, and using similar interpolations, Villain (1951) published a chart for M_2 over all the oceans which uses all the known harmonic constants. There is little doubt that as additional data become available new and more accurate charts of this kind will appear. While such charts may give a good estimate for the phase of the tides, they only provide a rough approximation for the amplitude, particularly in the regions very remote from the coasts.

Defant (1924) applied dynamical treatment to the spring tides of the Atlantic and Arctic Oceans, regarding these oceans as a single basin. He considered two phases of longitudinal oscillation, one being a forced vibration and the other a co-oscillation with the waters of the Southern Ocean. Later, in 1932, he revised the work and restricted it to the central line of that part of the ocean lying to the south of Iceland, where he assumed that the rotation of the earth would have little effect on the tides and the dissipation of energy would be small.

In 1944 Proudman examined the distribution of M_2 in the section of the Atlantic between 35° S and 45° N, allowing for the rotation of the earth but neglecting the dissipation of energy. Taking arbitrary values of current and elevation along the 35° S parallel, he considered a forced oscillation due to the tide-generating forces and four free oscillations in the form of north- and south-going Kelvin and Poincaré waves. He then took linear combinations of these oscillations to give agreement with observed values of M_2 at four different stations on the coastal boundaries.

Hansen (1949) used a different technique in his investigation of the semi-diurnal tides in the North Atlantic. Taking conditions at a number of 'boundary' stations he applied them to a system of approximate equations derived from the fundamental tidal equations. He was able to deduce the tides at a network of points at intervals across the ocean, ultimately combining these values in two co-level charts.

Proudman enunciated a theorem in tidal dynamics in 1925 which outlined a method whereby tidal elevations at points away from the coasts might be calculated if the coastal values were known. The work which follows applies this theorem to the equatorial distribution of the constituent K_2 across the Indian Ocean. In this work the depth of the ocean has been taken as uniform except in certain coastal areas where special corrections have been applied. This is the first application of the theorem, and it is also believed to be the first *direct* arithmetical calculation of oceanic tidal distribution.

2. THE TIDAL THEOREM

The following notation will be used:

- a the radius of the earth
 ω the angular speed of the earth's rotation
 g the acceleration due to gravity
 h the depth of water below any point in the mean surface
 h_1 the mean depth of the Indian Ocean north of the equator excluding the Andaman Basin
 $\beta = \frac{4\omega^2 a^2}{gh_1}$
 θ, χ the co-latitude and east longitude of any point, $\chi = 0$ being at 43° E, where the equator strikes the coast of Africa
 t the time measured from the instant of high water of the equilibrium constituent on meridian $\chi = 32^\circ$
 ζ the elevation of the free surface of the water at any time above any point of the mean surface
 $\bar{\zeta}$ the equilibrium elevation corresponding to the astronomical disturbing forces
 σ the angular speed of a harmonic tidal constituent
 u, v, ν the mean values along any vertical of the velocity components at any time in the directions of increasing θ and χ and along the outward normal to a section respectively
 U, V, Z mathematical functions satisfying differential equations similar to those for tidal motion
 N the component along the outward normal to a boundary section of the vector whose components in the directions of increasing θ and χ are U and V respectively.

It is also convenient to write $\zeta' = \zeta - \bar{\zeta}$.

A complex harmonic tidal constituent is used where time enters solely through the factor $e^{i\sigma t}$. Only the real parts of the function are interpreted. In the constituent $\zeta = (\zeta_1 + i\zeta_2) e^{i\sigma t}$ the real part is $\zeta_1 \cos \sigma t - \zeta_2 \sin \sigma t$. The equilibrium elevation is used in the form

$$\bar{\zeta} = \bar{H} \exp \left\{ 2i \left(\chi + \omega t - \frac{8}{45} \pi \right) \right\} \sin^2 \theta.$$

With spherical co-ordinates the equation of continuity is

$$\frac{1}{a \sin \theta} \left\{ \frac{\partial}{\partial \theta} (h \sin \theta u) + \frac{\partial}{\partial \chi} (h v) \right\} + i\sigma \zeta = 0. \quad (1)$$

If frictional forces and vertical accelerations are ignored the equations of motion are

$$i\sigma u - 2\omega \cos \theta v = -g \frac{\partial \zeta'}{a \partial \theta}, \quad (2)$$

$$i\sigma v + 2\omega \cos \theta u = -g \frac{\partial \zeta'}{a \sin \theta \partial \chi}. \quad (3)$$

U , V and Z are analogous to the elements in a free type of motion, being auxiliary complex functions of θ and χ satisfying the equations

$$\frac{1}{a \sin \theta} \left\{ \frac{\partial}{\partial \theta} (h \sin \theta U) + \frac{\partial}{\partial \chi} (hV) \right\} + i\sigma Z = 0, \quad (4)$$

$$i\sigma U + 2\omega \cos \theta V = -g \frac{\partial Z}{a \partial \theta}, \quad (5)$$

$$i\sigma V - 2\omega \cos \theta U = -g \frac{\partial Z}{a \sin \theta \partial \chi}. \quad (6)$$

For a region of the ocean, application of Green's theorem gives

$$\int h v ds = \iint \frac{1}{a \sin \theta} \left\{ \frac{\partial}{\partial \theta} (h \sin \theta u) + \frac{\partial}{\partial \chi} (h v) \right\} dS, \quad (7)$$

where ds and dS are boundary and surface elements respectively. If u , v and v are replaced by $\zeta'U$, $\zeta'V$ and $\zeta'N$ in (7) then substitution from (4), (5) and (6) gives

$$\int h \zeta' N ds = -i\sigma \iint \zeta' Z dS - \frac{1}{g} \iint h \{ i\sigma (Uu + Vv) - 2\omega \cos \theta (Uv - Vu) \} dS. \quad (8)$$

Similarly substitution in (7) from equations (1), (5) and (6) yields the relation

$$\int h Z v ds = -i\sigma \iint Z \zeta dS - \frac{1}{g} \iint h \{ i\sigma (uU + vV) + 2\omega \cos \theta (uV - vU) \} dS. \quad (9)$$

Subtraction of (9) from (8) gives

$$\int h \zeta' N ds - \int h Z v ds = i\sigma \iint \zeta Z dS. \quad (10)$$

Except for the neglect of frictional forces this is identical with the theorem in tidal dynamics as given by Proudman.

3. APPLICATION OF THE TIDAL THEOREM

An ocean bounded partly by an unbroken coastline and partly by a chord AB is shown in figure 1, in which C represents an island within the region. From the theorem the tidal elevation along AB may be deduced if the elevation along the coast is known. The method has the great advantage that allowance can be made for islands.

If ζ' is replaced by its components in (10)

$$\int h (\zeta - \bar{\zeta}) N ds = \int h Z v ds + i\sigma \iint \bar{\zeta} Z dS. \quad (11)$$

If Z is chosen so that $Z = 0$ along AB then $\int h Z v ds$ is zero, since $h v$ is zero along the coast. Hence

$$\int h (\zeta - \bar{\zeta}) N ds = i\sigma \iint \bar{\zeta} Z dS. \quad (12)$$

On the coast, including that of the island, the actual elevation ζ can be obtained from observations and the distribution of ζ may be calculated from astronomical and geographical data. The depth h can be found from bathymetric charts and the auxiliary functions computed. Thus a value can be deduced for $\int h\zeta N ds$ along the line AB .

The particular case where AB is part of a parallel of latitude may be taken. Where hN is independent of longitude the integral becomes $hN \int \zeta ds$. Consequently, a mean value for the elevation along AB is obtainable. If hN varies according to $\cos m\chi$, where the longitude of A is zero and that of B is π/m , it is possible to calculate a coefficient of a Fourier cosine series for ζ along AB . Further coefficients in this series may be found by using successive multiples of m as described later.

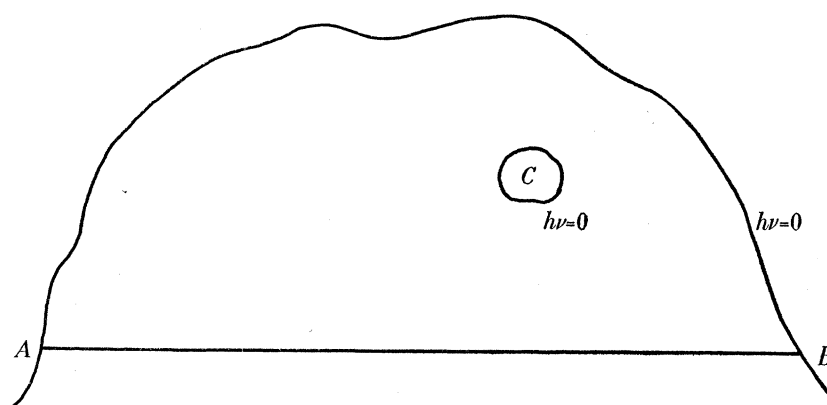


FIGURE 1. An oceanic region bounded by a chord.

The theorem was applied to the northern part of the Indian Ocean in an attempt to find the distribution of the semi-diurnal tidal constituent K_2 along the equator. This area seemed quite suitable since its coast-line is unbroken except for the relatively narrow entrances to the Red Sea, the Persian Gulf and the Malacca Strait. In the first two instances boundaries were taken across the narrowest parts of the Gulf of Aden and the Gulf of Oman respectively (figure 6), and currents across these boundaries were neglected. Owing to the shallow-water effects, it was found necessary to exclude the Strait of Malacca and the Andaman Basin. An arbitrary boundary passing through the Andaman Islands was taken along the oceanic side of the basin. The currents across this extensive water barrier could not be ignored, so it was essential to return to equation (11) and consider $\int hZ\nu ds$, the boundary integral containing the normal component of current. Unfortunately, knowledge of the currents near the Andaman Basin was inadequate for direct integration. It was possible, however, to convert the integral into a form which could be readily evaluated and this was used as a 'correction term' to be added to the simplified equation (12).

Use of the constituent K_2 was advantageous because its angular speed is exactly twice that of the earth's rotation, thus permitting appreciable simplification of the dynamical equations. Further simplification was achieved by taking a uniform depth for the enclosed ocean. Exclusion of the relatively shallow Andaman Basin and adjustments to the tidal

data in the shallow-water regions off the coasts of India and Burma decreased the probability of large errors arising from this approximation.

Now in (12), $N = U$ and $\delta s = a \delta \chi$ along the equator, $\delta S = a^2 \sin \theta \delta \theta \delta \chi$, and for coastal elements away from the equator $N \delta s = -U a \sin \theta \delta \chi + V a \delta \theta$. If \int_E , \int_C and \iint_O denote integrals along the equator, along the coast and over the surface of the ocean respectively, then equation (12) gives

$$\int_E h_1(\zeta - \bar{\zeta}) U a d\chi + \int_C h_1(\zeta - \bar{\zeta}) (-U a \sin \theta d\chi + V a d\theta) = i\sigma \iint_O \bar{\zeta} Z a^2 \sin \theta d\theta d\chi. \quad (13)$$

Where the 'coastal' integral includes a water boundary of length l a correction term $\int_l h_1 Z \nu ds$ must be added to the right-hand side of the equation.

4. THE USE OF AUXILIARY FUNCTIONS INDEPENDENT OF LONGITUDE

To evaluate the integrals in equation (13) it is first necessary to determine the auxiliary functions. The equations defining these functions assume a relatively simple form for K_2 in an ocean of constant depth h_1 . The condition that the functions are independent of longitude allows expressions to be found for them in terms of θ , ω , g , h_1 and a . Immediate substitution can be made in (13) yielding integrals which may be readily evaluated.

If $h = h_1$ and $\sigma = 2\omega$ are substituted in equations (4), (5) and (6) and if auxiliary functions independent of χ are taken then

$$\frac{h_1}{2\omega a \sin \theta} \frac{d}{d\theta} (U \sin \theta) + iZ = 0, \quad (14)$$

$$\frac{2\omega a}{g} (iU + V \cos \theta) = -\frac{dZ}{d\theta}, \quad (15)$$

$$\frac{2\omega a}{g} (iV - U \cos \theta) = 0. \quad (16)$$

Elimination of V from (15) and (16) gives

$$\frac{2\omega a}{g} iU(1 - \cos^2 \theta) = -\frac{dZ}{d\theta}. \quad (17)$$

If the variable is changed by putting $\cos \theta = \mu$, then equations (14) and (17) become

$$\frac{h_1}{2\omega a} \frac{d}{d\mu} (U \sin \theta) = iZ, \quad (18)$$

$$\frac{2\omega a}{g} iU \sin \theta = \frac{dZ}{d\mu}. \quad (19)$$

It therefore follows that

$$\frac{d^2 Z}{d\mu^2} = -\beta Z, \quad (20)$$

where

$$\beta = \frac{4\omega^2 a^2}{gh_1}.$$

This relation was first given by Doodson (1928) in an investigation into the application of numerical methods of integration to tidal dynamics. Taking $Z = 0$ on the equator, where $\mu = 0$, a solution for (20) is

$$Z = \sin(\beta^{\frac{1}{2}}\mu). \quad (21)$$

Reversion to the original notation, where μ is replaced by $\cos\theta$, enables U and V to be obtained by substitution for Z in equation (19) and for U in equation (16). Hence

$$U = -\frac{i(g/h_1)^{\frac{1}{2}} \cos(\beta^{\frac{1}{2}} \cos \theta)}{\sin \theta},$$

$$V = -\left(\frac{g}{h_1}\right)^{\frac{1}{2}} \cot \theta \cos(\beta^{\frac{1}{2}} \cos \theta),$$

$$Z = \sin(\beta^{\frac{1}{2}} \cos \theta).$$

If substitution is made for σ , U , V and Z in equation (13) and the correction term added

$$\int_E \zeta d\chi = \int_E \bar{\zeta} d\chi + \int_C (\zeta - \bar{\zeta}) \cos(\beta^{\frac{1}{2}} \cos \theta) (d\chi + i \cot \theta d\theta) - \beta^{\frac{1}{2}} \iint_O \bar{\zeta} \sin(\beta^{\frac{1}{2}} \cos \theta) \sin \theta d\theta d\chi - \frac{1}{ia(g h_1)^{\frac{1}{2}}} \int_l h_1 Z \nu ds. \quad (22)$$

The integrals on the right-hand side of this equation can all be evaluated if the entire distribution of $\bar{\zeta}$ and the coastal distribution of ζ are known. The sum of the various integrals gives $\int_E \zeta d\chi$; hence ζ_0 , the mean equatorial elevation, may be deduced.

5. THE USE OF AUXILIARY FUNCTIONS CONTAINING A FACTOR $e^{im\chi}$

As above, the auxiliary functions are found from the original definitions. If the functions have a common factor $e^{im\chi}$, then equations (4), (5) and (6) may be written

$$\frac{h_1}{2\omega a \sin \theta} \left\{ \frac{\partial}{\partial \theta} (U \sin \theta) + imV \right\} + iZ = 0, \quad (23)$$

$$\frac{2\omega a}{g} (iU + V \cos \theta) = -\frac{\partial Z}{\partial \theta}, \quad (24)$$

$$\frac{2\omega a}{g} (iV - U \cos \theta) = -\frac{imZ}{\sin \theta}. \quad (25)$$

When the following changes in variable are made

$$\frac{\beta}{2\omega a} U = -\frac{iU_m}{\sin \theta} e^{im\chi}, \quad (26)$$

$$\frac{\beta}{2\omega a} V = -\frac{V_m}{\sin \theta} e^{im\chi}, \quad (27)$$

$$\frac{Z}{h_1} = Z_m e^{im\chi}, \quad (28)$$

the previous equations become

$$\frac{1}{\sin \theta} \frac{dU_m}{d\theta} + \frac{mV_m}{\sin^2 \theta} - \beta Z_m = 0, \quad (29)$$

$$U_m - V_m \cos \theta = -\sin \theta \frac{dZ_m}{d\theta}, \quad (30)$$

$$-V_m + U_m \cos \theta = -mZ_m. \quad (31)$$

In equations (23), (24) and (25) U and V had the dimensions of currents and Z that of length, whereas in (29), (30) and (31) U_m , V_m and Z_m are dimensionless.

Substitution of $\mu = \cos \theta$ in the above equations gives

$$\frac{dU_m}{d\mu} = \frac{mV_m}{1-\mu^2} - \beta Z_m, \quad (32)$$

$$(1-\mu^2) \frac{dZ_m}{d\mu} = U_m - \mu V_m, \quad (33)$$

$$V_m = mZ_m + \mu U_m. \quad (34)$$

Elimination of V_m from (32) and (33) gives

$$\frac{dU_m}{d\mu} = \frac{m\mu}{(1-\mu^2)} U_m + \left(\frac{m^2}{1-\mu^2} - \beta \right) Z_m, \quad (35)$$

$$(1-\mu^2) \frac{dZ_m}{d\mu} = (1-\mu^2) U_m - m\mu Z_m. \quad (36)$$

With initial known values of U_m and Z_m on the equator this pair of equations may be integrated over the required range of μ using step-by-step methods. For the values of U_m and Z_m obtained after each increment the equivalent values of V_m may be calculated from (34). If $Z_m = 0$ on the equator then any suitable value may be assigned to U_m . As shown below it is convenient to take $U_m = \frac{1}{2}$.

When the correction term has been added to equation (13) substitution for U , V and Z from the relations (26), (27) and (28) gives

$$\begin{aligned} U_E \int_E (\zeta - \bar{\zeta}) e^{im\chi} d\chi - \int_C (\zeta - \bar{\zeta}) \left(U_m e^{im\chi} d\chi + \frac{iV_m}{\sin \theta} e^{im\chi} d\theta \right) \\ = -\beta \iint_O \bar{\zeta} Z_m e^{im\chi} \sin \theta d\theta d\chi - \frac{\beta}{2i\omega a^2} \int_l h_1 \nu Z_m e^{im\chi} ds, \end{aligned} \quad (37)$$

where U_E is the value of U_m on the equator. Replacement of m by $-m$ and use of the same equatorial value of U_m yields

$$\begin{aligned} U_E \int_E (\zeta - \bar{\zeta}) e^{-im\chi} d\chi - \int_C (\zeta - \bar{\zeta}) \left(U_{-m} e^{-im\chi} d\chi + \frac{iV_{-m}}{\sin \theta} e^{-im\chi} d\theta \right) \\ = -\beta \iint_O \bar{\zeta} Z_{-m} e^{-im\chi} \sin \theta d\theta d\chi - \frac{\beta}{2i\omega a^2} \int_l h_1 \nu Z_{-m} e^{-im\chi} ds. \end{aligned} \quad (38)$$

If (37) and (38) are added, and if $U_E = \frac{1}{2}$ then

$$\begin{aligned} \int_E (\zeta - \bar{\zeta}) \cos m\chi d\chi - \int_C (\zeta - \bar{\zeta}) (U_m e^{im\chi} + U_{-m} e^{-im\chi}) d\chi - \int_C (\zeta - \bar{\zeta}) \left(\frac{iV_m}{\sin \theta} e^{im\chi} + \frac{iV_{-m}}{\sin \theta} e^{-im\chi} \right) d\theta \\ = -\beta \iint_O \bar{\zeta} (Z_m e^{im\chi} + Z_{-m} e^{-im\chi}) \sin \theta d\theta d\chi - \frac{\beta}{2i\omega a^2} \int_l h_1 \nu (Z_m e^{im\chi} + Z_{-m} e^{-im\chi}) ds. \end{aligned} \quad (39)$$

From this equation the coefficient of a term in a cosine series for ζ can be found if the equatorial longitude extends over the range 0 to π/m radians. If successive integral multiples of m be then used in the exponential factor, further groups of auxiliary functions may be computed. Hence additional Fourier coefficients may be calculated giving a better approximation for the distribution of the tidal constituent.

6. MEAN DEPTH OF THE INDIAN OCEAN NORTH OF THE EQUATOR

The mean depth was found from the most recent edition of the *General bathymetric chart of the oceans*, issued by the International Hydrographic Bureau. Sections AIII (1940) and AIV (1938) of the third edition of the chart were divided into rectangles bounded by 1° of latitude and 1° of longitude. For each rectangle, or fraction of a rectangle, the depth was estimated to the nearest 50 m. Despite the large number of soundings on the chart a considerable amount of interpolation was needed in areas remote from the coasts. As previously stated the Andaman Basin was excluded, the arbitrary boundary being that shown in figure 4. The mean depth of the remaining area was estimated to be 3200 m, approximating to the nearest 100 m.

With this value for h_1 it was now possible to calculate β . If $\omega = 7.293 \times 10^{-5} \text{ s}^{-1}$, $a = 6.37 \times 10^6 \text{ m}$ and $g = 9.80 \text{ m s}^{-2}$;

$$\beta = \frac{4\omega^2 a^2}{gh_1} = 27.5313.$$

7. COMPUTATION OF AUXILIARY FUNCTIONS FOR $\pm m, \pm 2m, \pm 3m$

A method for computation of auxiliary functions of this type was given by Doodson (1928), but in the present work method II of Fox & Goodwin (1948) was employed. A recurrence relation was deduced from the first-order equations (35) and (36), the relation being based on the formula

$$y_1 = y_0 + \frac{1}{2}k(\dot{y}_0 + \dot{y}_1) + \Delta(y), \quad (40)$$

$$\Delta(y) = \left(-\frac{1}{12}\delta^3 + \frac{1}{120}\delta^5 - \frac{1}{840}\delta^7 + \dots\right) y_1. \quad (41)$$

In the formula, y_0 and y_1 are the values of y at successive points in the range of integration, with an interval k between them. \dot{y}_0 and \dot{y}_1 are the derivatives of y_0 and y_1 respectively. The error term, $\Delta(y)$, is expressed as an infinite series of central differences in (41).

Equations (35) and (36) may be written

$$\dot{U}_m = fU_m + bZ_m, \quad (42)$$

$$\dot{Z}_m = U_m - fZ_m, \quad (43)$$

where

$$f = \frac{m\mu}{1-\mu^2} \quad \text{and} \quad b = \left(\frac{m^2}{1-\mu^2} - \beta\right).$$

Let $U_{m,0}, U_{m,1}, U_{m,2}, \dots$ be successive values of U_m taken at intervals k over the range of integration, and let the corresponding values of Z_m, f and b be $Z_{m,0}, Z_{m,1}, Z_{m,2}, \dots, f_0, f_1, f_2, \dots$ and b_0, b_1, b_2, \dots , respectively. Application of (40) to equations (42) and (43) gives

$$\begin{aligned} (1 - \frac{1}{2}kf_1) U_{m,1} - \frac{1}{2}kb_1 Z_{m,1} &= (1 + \frac{1}{2}kf_0) U_{m,0} + \frac{1}{2}kb_0 Z_{m,0} + \Delta(U_m), \\ -\frac{1}{2}kU_{m,1} + (1 + \frac{1}{2}kf_1) Z_{m,1} &= \frac{1}{2}kU_{m,0} + (1 - \frac{1}{2}kf_0) Z_{m,0} + \Delta(Z_m). \end{aligned}$$

Hence

$$\begin{aligned} U_{m,1} [1 - \frac{1}{4}k^2(f_1^2 + b_1)] &= [1 + \frac{1}{2}k(f_0 + f_1) + \frac{1}{4}k^2(f_0 f_1 + b_1)] U_{m,0} \\ &\quad + (1 + \frac{1}{2}kf_1) \Delta(U_m) + \frac{1}{2}kb_1 \Delta(Z_m) + \frac{1}{2}k[(b_0 + b_1) + \frac{1}{2}k(f_1 b_0 - f_0 b_1)] Z_{m,0}, \\ Z_{m,1} [1 - \frac{1}{4}k^2(f_1^2 + b_1)] &= \frac{1}{2}k[2 + \frac{1}{2}k(f_0 - f_1)] U_{m,0} + \frac{1}{2}k \Delta(U_m) \\ &\quad + (1 - \frac{1}{2}kf_1) \Delta(Z_m) + [1 - \frac{1}{2}k(f_0 + f_1) + \frac{1}{4}k^2(f_1 f_0 + b_0)] Z_{m,0}. \end{aligned}$$

If $\Delta(U_m)$ and $\Delta(Z_m)$ are neglected these equations may be written

$$KU_{m,1} = AU_{m,0} + BZ_{m,0}, \quad (44)$$

$$KZ_{m,1} = CU_{m,0} + DZ_{m,0}, \quad (45)$$

where
$$K = 1 - \frac{1}{4}k^2(f_1^2 + b_1), \quad A = 1 + \frac{1}{2}k(f_0 + f_1) + \frac{1}{4}k^2(f_0f_1 + b_1),$$

$$B = \frac{1}{2}k[(b_0 + b_1) + \frac{1}{2}k(f_1b_0 - f_0b_1)], \quad C = k + \frac{1}{4}k^2(f_0 - f_1)$$

and
$$D = 1 - \frac{1}{2}k(f_0 + f_1) + \frac{1}{4}k^2(f_1f_0 + b_0).$$

The enclosed part of the ocean lies between 0 and 27° N, and the equator extends over 56·6° of longitude. Thus $0 \leq \mu \leq 0.454$ and $m = 3.18$. To simplify interpolation of the functions when they were used in the integrals the interval k was taken as 0.01. K, A, B, C and D were tabulated for $\pm m, \pm 2m$ and $\pm 3m$. With $U_{m,0} = 0.5$ and $Z_{m,0} = 0$, approximate values of the variables were found over the whole range of integration by means of equations (44) and (45). The process was repeated for the multiples of m , using the same pair of initial values. All these values were differenced and the error terms obtained by applying equation (41). The step-by-step integration was now repeated, making allowance for the error terms, and in all cases a sufficient degree of accuracy was produced. With higher multiples of m it would, however, have been necessary to repeat the differencing and integration processes at least once more. The functions were calculated correct to four places of decimals, two guarding figures being retained during the computational processes to reduce 'building-up' errors. The appropriate values of the third function were found by use of equation (34).

To check the accuracy of the entire computation a series solution was obtained for the original differential equations (35) and (36).

Taking

$$Z_m = c_1\mu + c_3\mu^3 + c_5\mu^5 + c_7\mu^7 + \dots,$$

$$U_m = \frac{1}{2} + a_2\mu^2 + a_4\mu^4 + a_6\mu^6 + \dots,$$

the following relations were deduced between the coefficients

$$(2r+1)c_{2r+1} = a_{2r} - a_{2r-2} + (2r-1-m)c_{2r-1}, \quad (46)$$

$$2ra_{2r} = (2r-2+m)a_{2r-2} + (m^2 - \beta)c_{2r-1} + \beta c_{2r-3}. \quad (47)$$

Sufficient coefficients were calculated to enable U_m and Z_m to be found, correct to four places of decimals, after every tenth stage of the numerical integration. With $\pm m$ this check was relatively easy, but for multiples of m the coefficients increased rapidly (table 1).

A table giving values of the auxiliary functions, computed at intervals of 0.01 over the range $0 \leq \mu \leq 0.45$, has been deposited in the archives of the Royal Society. Most of the outstanding characteristics of the functions may be seen in table 2, where values of U, V and Z are given at the extremities and near the centre of the range of integration.

For $+m$, U decreases with increasing μ , i.e. with increasing latitude, while V and Z increase initially and then diminish, their maxima being 0.4131 and 0.1113 respectively. For $-m$, U and V both decrease away from the equator, while Z increases. With $2m$ and $3m$ all the functions increase with latitude and with $-2m$ and $-3m$ both U and V increase and Z decreases in value.

The outstanding characteristic of all the functions is their rapid increase in numerical value for higher multiples of m , especially in the higher latitudes. This behaviour is most easily explained by reference to the recurrence relations (46) and (47). The most important coefficient is $(m^2 - \beta)$, which is present in (47). For m , $2m$ and $3m$ this coefficient has values $-17\cdot419$, $12\cdot918$ and $63\cdot480$ respectively. With the last two values the coefficients in the series solutions for the functions U and Z are all positive and increase in value, as may be seen in the examples quoted to the nearest integer in table 1. For higher multiples of m the coefficients would be much larger, producing correspondingly greater values in U and Z .

TABLE 1. COEFFICIENTS IN THE SERIES SOLUTION FOR THE AUXILIARY FUNCTIONS, GIVEN TO THE NEAREST INTEGER

coeff.	m	$-m$	$2m$	$-2m$	$3m$	$-3m$
c_5	2	2	2	4	16	27
a_6	-6	-9	33	13	477	250
c_9	0	0	3	12	80	194
a_{10}	-1	-1	96	41	2888	1358
c_{19}	—	—	8	60	672	2845
a_{20}	—	—	436	192	37968	16326

TABLE 2. REPRESENTATIVE VALUES OF THE AUXILIARY FUNCTIONS

function	μ	m	$-m$	$2m$	$-2m$	$3m$	$-3m$
U	0	0.5000	0.5000	0.5000	0.5000	0.5000	0.5000
	0.25	0.3006	0.2156	0.8699	0.6329	2.2781	1.7064
	0.45	-0.0102	-0.1928	2.5200	1.2865	17.1412	10.1642
V	0	0	0	0	0	0	0
	0.25	0.3935	-0.2894	1.0784	-0.8248	2.6071	-1.9849
	0.45	0.3189	-0.5431	3.1555	-2.5223	18.8664	-12.9167
Z	0	0	0	0	0	0	0
	0.25	0.1001	0.1080	0.1354	0.1546	0.2136	0.2528
	0.45	0.1017	0.1435	0.3178	0.4876	1.1691	1.8334

8. TIDAL DATA

Harmonic constants for the constituent K_2 at various coastal stations were obtained from the *List of harmonic constants* published by the International Hydrographic Bureau (1931 and later).

The phase angles were given in the forms κ or g , and it was necessary to adjust them for a standard meridian and time. This was achieved by application of the formulae

$$g = \kappa + 2L - \sigma T \quad \text{and} \quad g_1 - g = \sigma(T - T_1).$$

In these equations

κ is the phase lag of the tidal constituent behind the phase of the corresponding equilibrium constituent at the place;

L is the longitude of the station in degrees west of Greenwich;

σ is the angular speed of the constituent in degrees per mean solar hour (i.e. $30\cdot082\text{h}^{-1}$ for K_2);

the time is measured in standard time T hours later than Greenwich mean time;

the second equation allows for a change in the time meridian from T to T_1 ;

standard time was taken with $T_1 = -5\cdot5\text{h}$, i.e. $5\cdot5\text{h}$ fast with respect to Greenwich; the phase lag g_1 was calculated for each station and these values, together with the amplitudes are shown in table 3.

Use of this standard meridian, and omission of the time factor gives

$$\bar{\zeta} = \bar{H} e^{2i(\chi - \frac{8}{45}\pi)} \sin^2 \theta,$$

where H , calculated from astronomical data, has the value 3.08 cm. Similarly $\zeta = H e^{-ig_1}$.

TABLE 3. VALUES OF HARMONIC CONSTANTS H AND g_1 AT COASTAL STATIONS

station number	station	H (cm)	g_1 (deg.)	station number	station	H (cm)	g_1 (deg.)
1	Chisimaio	10.9	217	30	Colombo	3.3	081
2	Mogadiscio	7.7	218	31	Galle	3.4	085
3	Obbia	7.2	218	32	Trincomali	2.0	242
4	Berbera	5.5	307	33	Point Pedro	2.4	255
5	Djibouti	6.0	303	34	Jaffna	1.5	108
6	Perim	5.0	295	35	Madras	3.6	258
7	Aden	5.7	300	36	Cocanada	5.2	270
8	Maskat	6.2	332	37	Vizagapatam	5.9	261
9	Kuwai	6.7	021	38	False Point	8.3	276
10	Karachi	8.2	335	39	Shortt Island	12.6	288
11	Navinar Point	11.3	074	40	Dublat Saugor	19.0	298
12	Kandla Harbour	19.8	096	41	Chittagong	13.1	033
13	Hansthal Point	16.1	091	42	Akyab	9.8	272
14	Navlaki	18.3	090	43	Diamond Island	8.1	271
15	Okha Point	9.9	026	44	Elephant Point	22.9	095
16	Porbandar	6.3	334	45	Amherst	30.1	051
17	Port Victor Albert	8.1	084	46	Moulmein	12.5	101
18	Bhaunagar	26.6	177	47	Mergui	25.6	297
19	Bombay	12.2	343	48	Sir E. Owen Island	16.5	291
20	Murmagao	5.7	326	49	Sullivan Island	17.7	287
21	Karwar	5.3	331	50	Pulau Besin	15.8	283
22	Mangalore	1.8	349	51	Ao Kaulak	9.4	274
23	Beypore	2.6	008	52	Pulau Kapai	11.9	292
24	Ponnani	3.0	021	53	North Cone Island	12.2	298
25	Cochin	2.4	020	54	Penang	9.5	330
26	Quilon	3.0	069	55	Port Blair	7.9	273
27	Tuticorin	3.9	077	56	Pulau Rusa	2.0	253
28	Pamban Pass	3.4	082	57	Chalang Bay	2.0	205
29	Negapatam	2.6	276	58	Mulaboh	2.0	211
				59	Singkel	3.0	177
				60	Gunung Sitoli	5.0	355
				61	Natal	3.0	166

9. INTERPOLATED VALUES OF THE HARMONIC CONSTANTS

The coastal area was considered in rectangles bounded by the lines denoting degrees of latitude and longitude. Representative values of H and g_1 were given to the strip of coastline lying within each rectangle. A table giving these values has been deposited in the archives of the Royal Society.

Several problems were encountered in the interpolation due to the comparatively small list of harmonic constants, and, to a much greater extent, to the presence of large areas of shallow water along the north-west coast of India, the Bay of Bengal and the Malay Peninsula.

From the map shown in figure 6 it will be seen that there are large intervals between Obbia and Berbera, Aden and Maskat, and Kuwai and Karachi where no harmonic constants are yet available. In each of these regions extensive information was found in the *Admiralty tide tables*, part II (1938), for the constituent M_2 . The distribution of this constituent shows

more or less regular changes in amplitude and phase, both of quite small magnitude. The known constants for K_2 indicate a similar type of distribution and interpolation was carried out on this assumption.

Between Karachi and Murmagao several stations have very large amplitudes and widely different phase angles, notably in the Gulfs of Kutch and Cambay. The large amplitudes are almost certainly due to the broad shelf of very shallow water off the coast, in conjunction with the shape of the coastline. A uniform depth h_1 having been taken for the enclosed ocean it was necessary to replace the excessively large values of H by others more appropriate for this depth. The high amplitudes within the Gulfs were ignored and H was plotted against distance for stations between Karachi and Karwar, which lies to the south of Murmagao. A smooth curve was drawn passing through the points provided by Karachi, Murmagao and Karwar, where the values seem to be satisfactory for oceanic depths. The curve, shown in figure 2, was used as a basis for interpolation over the region. This part of

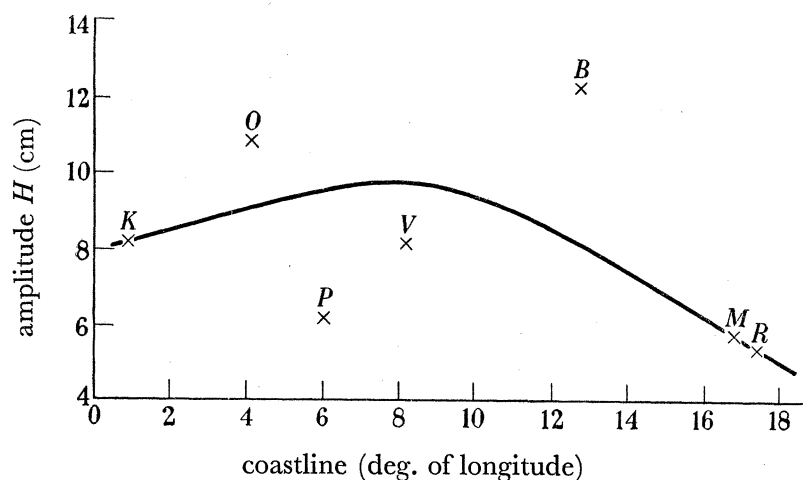


FIGURE 2. Amplitude variations between Karachi and Karwar. *K*, Karachi; *O*, Okhar Point; *P*, Porbandar; *V*, Port Victor Albert; *B*, Bombay; *M*, Murmagao; *R*, Karwar.

the coastline being remote from the equator the auxiliary functions for it are large compared with those near the equator, especially for higher multiples of m . Since the amplitude H is also large the contributions to the coastal integrals are relatively important. As explained in §12 a few of the interpolated values of H were slightly adjusted and the numerical integration repeated after the initial summation of these integrals. The modifications were introduced along the north-east and north-west coasts of India, and the greatest changes in H and g_1 were 1.5 cm and 5° respectively.

At the head of the Bay of Bengal there is a further extensive shelf of shallow water, and once more the amplitude of the K_2 constituent is large. Here, however, the phase angles at the various stations have approximately the same magnitude. Consequently the tidal motion was treated as a 'co-oscillation in a narrow gulf' (Proudman 1953, §119), in an attempt to deduce amplitudes representative of oceanic depths.

If figure 3 represents a vertical section along the gulf the amplitude H_D in the region of transition from shallow to deep water is given by

$$H_D = H_A \cos \frac{\pi L}{l_1},$$

where H_A is the amplitude at the head of the gulf. The distance l_1 from the head of the gulf to the nodal point N may be found from the relation $l_1 = \frac{1}{2}T_2(gh_2)^{\frac{1}{2}}$, where T_2 is the period of the oscillation and h_2 the mean depth of the shelf of shallow water. If the amplitude at Dublat Saugor is taken as representative of the head of the Gulf,

$$H_A = 19.0 \text{ cm}, \quad T_2 = 12 \text{ h}, \quad L = 190 \text{ km} \quad \text{and} \quad h_2 = 70 \text{ m}.$$

Hence

$$l_1 = \frac{1}{2} \times 12 \text{ h} \times (9.81 \text{ m s}^{-2} \times 70 \text{ m})^{\frac{1}{2}} = 566 \text{ km}.$$

Thus

$$H_D = 19.0 \cos \frac{\pi \times 190}{566} \text{ cm} = 9.4 \text{ cm}.$$

H_D shows satisfactory agreement with observed values at 'oceanic' stations on both sides of the bay, namely, False Point (8.3 cm) and Diamond Island (8.1 cm). Accordingly, this value was accepted as an adequate estimate of the amplitude of K_2 in the absence of shallow water. Together with the two values mentioned above it was used for interpolation along this coastal region.

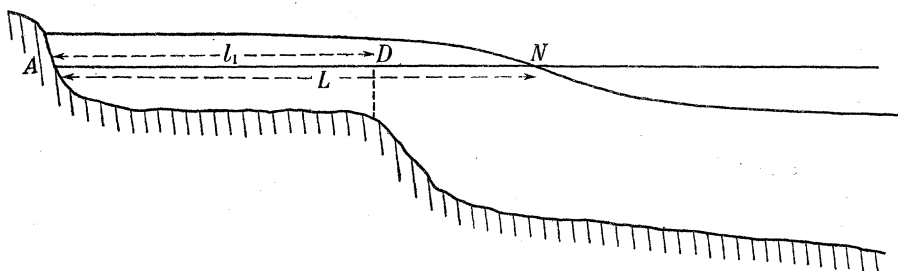


FIGURE 3. Vertical section showing a co-oscillation in the northern part of the Bay of Bengal.

Farther south in the Andaman Basin the water is extremely shallow near the coast and the amplitude of K_2 correspondingly large. The effect at various stations within the area (nos. 44 to 54) may be seen in table 3. In view of the magnitude of the area it was decided to exclude the whole basin, taking an arbitrary boundary passing through the Andaman Islands. Interpolation along the new boundary was effected by using the constants for K_2 at Diamond Island off the Burmese coast, at Port Blair in the Andaman Islands and at Pulau Rusa near Sumatra.

10. CORRECTIONS FOR THE ANDAMAN BASIN

Since an arbitrary boundary was used along the western side of the basin, as shown in figure 4, it was necessary to apply corrections to equations (22) and (39) to allow for the passage of water across the boundary. Little information could be found about the currents in this region, so an alternative approach had to be devised. From equation (12) the required correction is given by the term $\int_Q^P hZ\nu ds$. Now $\int h\nu ds = \frac{\partial}{\partial t} \iint \zeta dS$, thus providing a method for eliminating the current component ν . When mean values ζ_B , Z_B and θ_B are taken for the boundary, which encloses area A , then

$$\int_Q^P hZ\nu ds = Z_B \frac{\partial \zeta_B}{\partial t} A.$$

With $\zeta_B = H_B e^{2i\omega t - i g_B}$, $\frac{\partial \zeta_B}{\partial t} = 2i\omega H_B e^{2i\omega t - i g_B}$.

Since $\delta A = a^2 \sin \theta \delta \theta \delta \chi$, $A = a^2 \sin \theta_B \iint_A d\theta d\chi$.

The case involving functions independent of χ was considered first. The correction c required for the right-hand side of equation (22) is given by

$$-\frac{1}{ia(gh_1)^{\frac{1}{2}}} Z_B \frac{\partial \zeta_B}{\partial t} A,$$

which may be written

$$c = -\beta^{\frac{1}{2}} \sin \theta_B Z_B H_B (\cos g_B - i \sin g_B) \iint_A d\chi d\theta.$$

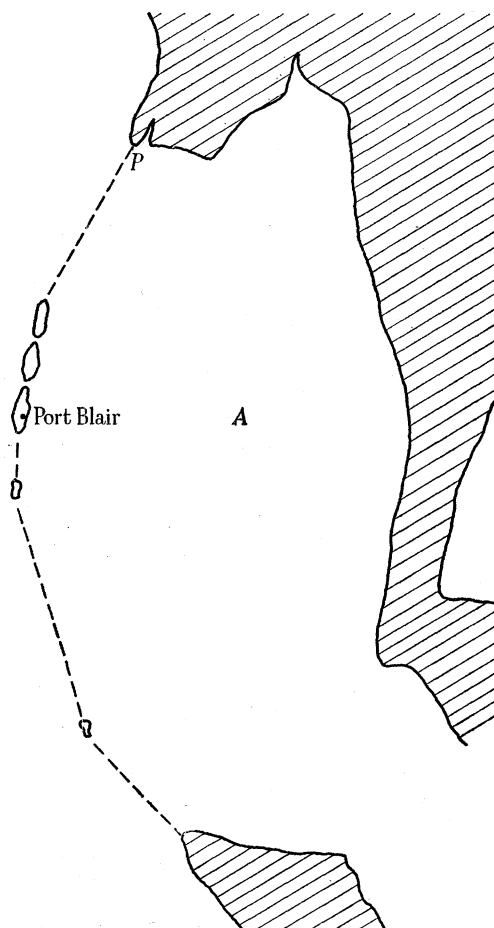


FIGURE 4. Arbitrary boundary along the Andaman Basin.

The harmonic constants at Port Blair were taken as typical values for the boundary, giving $H_B = 7.9$ cm and $g_B = 273^\circ$. If $\iint_A d\theta d\chi = 0.0188$, $\beta^{\frac{1}{2}} = 5.25$ and $\theta_B = 80^\circ$ then $Z_B = 0.7904$ and $c = -(0.03 + 0.61i)$ cm.

Where the auxiliary functions are dependent on longitude the correction c' must be applied to the right-hand side of equation (39). For $\pm m$

$$\begin{aligned} c' &= -\frac{\beta}{2i\omega a^2} (Z_m e^{im\chi_B} + Z_{-m} e^{-im\chi_B}) \times 2i\omega H_B a^2 \sin \theta_B (\cos g_B - i \sin g_B) \iint_A d\theta d\chi \\ &= -[(Z_m + Z_{-m}) \cos m\chi_B + i(Z_m - Z_{-m}) \sin m\chi_B] \beta H_B \sin \theta_B (\cos g_B - i \sin g_B) \iint_A d\theta d\chi. \end{aligned}$$

Z_m and Z_{-m} were both calculated at $\mu = \cos \theta_B$, χ_B was taken as $50 \cdot 5^\circ$ and the remaining numerical quantities were as before. Values of c' were found for m and its multiples and these are shown in table 5.

11. INTEGRATION

In the case where the auxiliary functions are independent of longitude, substitution for ζ and $\bar{\zeta}$ in equation (22) gives

$$\int_E \zeta d\chi = \bar{H} \int_E \exp \{2i(\chi - \frac{8}{45}\pi)\} d\chi + \int_C (H \exp \{-ig_1\} - \bar{H} \exp \{2i(\chi - \frac{8}{45}\pi)\} \sin^2 \theta) \cos(\beta^{\frac{1}{2}} \cos \theta) \times (d\chi + i \cot \theta d\theta) - \beta^{\frac{1}{2}} \bar{H} \iint_O \exp \{2i(\chi - \frac{8}{45}\pi)\} \sin(\beta^{\frac{1}{2}} \cos \theta) \sin^3 \theta d\theta d\chi.$$

The equatorial integral on the right-hand side was easily evaluated using the known coastal values of χ on the equator. The coastal integral involved a considerable amount of numerical work, since the coast was divided into approximately 150 sections. From the interpolation table for the harmonic constants, $H e^{-ig_1}$ was found for each section. Values of χ and θ were taken at the mid-point of each strip and $\bar{H} \exp \{2i(\chi - \frac{8}{45}\pi)\} \sin^2 \theta$, $\cos(\beta^{\frac{1}{2}} \cos \theta)$ and $\cot \theta$ were tabulated. With the appropriate increments $\delta\chi$ and $\delta\theta$ the computation was then carried out.

In the surface integral one stage of integration was performed directly since

$$\begin{aligned} -\beta^{\frac{1}{2}} \bar{H} \iint_O \exp \{2i(\chi - \frac{8}{45}\pi)\} \sin(\beta^{\frac{1}{2}} \cos \theta) \sin^3 \theta d\theta d\chi \\ = \frac{1}{2} i \beta^{\frac{1}{2}} \bar{H} \int_{\theta_1}^{\frac{1}{2}\pi} (e^{2i\chi_2} - e^{2i\chi_1}) \sin(\beta^{\frac{1}{2}} \cos \theta) \sin^3 \theta d\theta, \end{aligned}$$

where θ_1 is the most northerly value of θ and χ_1 and χ_2 are the values of $(\chi - \frac{8}{45}\pi)$ at the mid-points of the ends of a strip of ocean bounded by parallels of latitude $\delta\theta$ degrees apart. The remaining stage in the process was completed with one-degree increments in $\delta\theta$.

To these integrals was added the correction for the boundary of the Andaman Basin, derived in the previous paragraph. The integrals are all given in Table 4, where it will be seen that $\zeta_0 = -(1 \cdot 7 + 1 \cdot 1i)$ cm. Equation (39) may be written in the form

$$\begin{aligned} \int_E \cos m\chi d\chi = \bar{H} \int_E \exp \{2i(\chi - \frac{8}{45}\pi)\} \cos m\chi d\chi + \int_C (\zeta - \bar{\zeta}) [(U_m + U_{-m}) \cos m\chi \\ + i(U_m - U_{-m}) \sin m\chi] d\chi + \int_C (\zeta - \bar{\zeta}) \frac{i}{\sin \theta} [(V_m + V_{-m}) \cos m\chi + i(V_m - V_{-m}) \sin m\chi] d\theta \\ - \beta \bar{H} \iint_O [Z_m \exp \{i[(m+2)\chi - \frac{1}{45}\pi]\} + Z_{-m} \exp \{-i[(m-2)\chi + \frac{1}{45}\pi]\}] \sin^3 \theta d\theta d\chi. \end{aligned}$$

With m chosen so that the length of the boundary is π/m the first equatorial integral gave the value $\frac{\pi}{2m} \zeta_m$, where ζ_m is the coefficient of the term in $\cos m\chi$ in the Fourier series for ζ . The second equatorial integral was readily evaluated since

$$\begin{aligned} \bar{H} \int_E \exp \{2i(\chi - \frac{8}{45}\pi)\} \cos m\chi d\chi = \bar{H} \left[\frac{1}{m^2 - 4} \exp \{2i(\chi - \frac{8}{45}\pi)\} (2i \cos m\chi + m \sin m\chi) \right]_0^{\pi/m} \\ = \frac{\bar{H}}{m^2 - 4} [2i \cos 2(\chi - \frac{8}{45}\pi) \cos m\chi + m \cos 2(\chi - \frac{8}{45}\pi) \sin m\chi \\ - 2 \sin 2(\chi - \frac{8}{45}\pi) \cos m\chi + im \sin 2(\chi - \frac{8}{45}\pi) \sin m\chi]_0^{\pi/m}. \end{aligned}$$

The coastal integrals were found by numerical methods using the same increments as before, the various combinations of the auxiliary functions being obtained by linear interpolation. As in the former integral, corrections were eventually applied when the harmonic constants were modified in certain places.

TABLE 4. ζ_0 THE MEAN EQUATORIAL ELEVATION

integrals	(cm)	
	1	i
$\int_C (H \exp \{-ig_1\} - \bar{H} \exp \{2i(\chi - \frac{8}{45}\pi)\} \sin^2 \theta) \cos(\beta^{\frac{1}{2}} \cos \theta) d\chi$	-2.02	-0.51
$i \int_C (H \exp \{-ig_1\} - \bar{H} \exp \{2i(\chi - \frac{8}{45}\pi)\} \sin^2 \theta) \cos(\beta^{\frac{1}{2}} \cos \theta) \cot \theta d\theta$	0.12	0.02
$-\bar{H}\beta^{\frac{1}{2}} \iint_0 \exp \{2i(\chi - \frac{8}{45}\pi)\} \sin(\beta^{\frac{1}{2}} \cos \theta) \sin^3 \theta d\theta d\chi$	-2.32	0.35
$\bar{H} \int_E \exp \{2i(\chi - \frac{8}{45}\pi)\} d\chi$	2.55	-0.33
$-\beta^{\frac{1}{2}} \sin \theta_B Z_B H_B (\cos g_B - i \sin g_B) \iint_A d\theta d\chi$	-0.03	-0.61
$\int_E \zeta d\chi = 0.988\zeta_0$	-1.70	-1.08
ζ_0	-1.7	-1.1

TABLE 5. INTEGRALS AND FOURIER COEFFICIENTS FOR $n=m$, $2m$ AND $3m$

integrals	Values in cm					
	$n=m$		$n=2m$		$n=3m$	
	1	i	1	i	1	i
$\bar{H} \int_E \exp \{2i(\chi - \frac{8}{45}\pi)\} \cos n\chi d\chi$	-0.14	-1.09	-0.27	0.04	-0.01	-0.08
$\int_C (\zeta - \bar{\zeta}) (U_n + U_{-n}) \cos n\chi d\chi$	-0.29	0.96	-3.90	-0.11	-17.37	-10.77
$i \int_C (\zeta - \bar{\zeta}) (U_n - U_{-n}) \sin n\chi d\chi$	-0.35	0.16	-0.10	0.86	-1.91	-2.66
$i \int_C \frac{(\zeta - \bar{\zeta})}{\sin \theta} (V_n + V_{-n}) \cos n\chi d\theta$	0.27	0.12	0.14	-0.49	1.42	1.10
$-\int_C \frac{(\zeta - \bar{\zeta})}{\sin \theta} (V_n - V_{-n}) \sin n\chi d\theta$	-0.91	0.24	1.26	2.46	16.06	13.30
$\frac{i\beta\bar{H}}{n+2} \int_{\theta_1}^{\frac{1}{2}\pi} Z_n [\exp i\{(n+2)\chi_2 - \frac{1}{45}\pi\} - \exp i\{(n+2)\chi_1 - \frac{1}{45}\pi\}] \sin^3 \theta d\theta$	-0.18	-0.58	-0.11	-0.36	1.05	-0.81
$-\frac{i\beta\bar{H}}{n-2} \int_{\theta_1}^{\frac{1}{2}\pi} Z_{-n} [\exp -i\{(n-2)\chi_2 + \frac{1}{45}\pi\} - \exp -i\{(n-2)\chi_1 + \frac{1}{45}\pi\}] \sin^3 \theta d\theta$	0.17	1.48	1.30	0.02	0.98	-0.59
$-[(Z_n + Z_{-n}) \cos n\chi_B + i(Z_n - Z_{-n}) \sin n\chi_B] \times \beta H_B \sin \theta_B (\cos g_B - i \sin g_B) \iint_A d\theta d\chi$	0.03	0.55	-0.02	-0.52	0	0.43
$\int_E \zeta \cos n\chi d\chi = \frac{\pi}{2 \times 3.18} \zeta_n$	-1.40	1.84	-1.70	1.92	0.22	-0.08
ζ_n	-2.8	3.7	-3.4	3.9	0.4	-0.2

On integration with respect to χ the surface integral becomes

$$\begin{aligned}
 & + \frac{i\beta\bar{H}}{m+2} \int_{\theta_1}^{\frac{1}{2}\pi} Z_m [\exp \{i[(m+2)\chi_2 - \frac{1}{4}\frac{6}{5}\pi]\} - \exp \{i[(m+2)\chi_1 - \frac{1}{4}\frac{6}{5}\pi]\}] \sin^3 \theta d\theta \\
 & - \frac{i\beta\bar{H}}{m-2} \int_{\theta_1}^{\frac{1}{2}\pi} Z_{-m} [\exp \{-i[(m-2)\chi_2 + \frac{1}{4}\frac{6}{5}\pi]\} - \exp \{-i[(m-2)\chi_1 + \frac{1}{4}\frac{6}{5}\pi]\}] \sin^3 \theta d\theta.
 \end{aligned}$$

For the remaining stage the exponential terms were converted into the trigonometrical form and numerical integration carried out with one-degree increments in $\delta\theta$.

In table 5 the values of the integrals are given together with the correction for the Andaman Basin and the amplitude of the Fourier coefficient ζ_m . The series of integrations was repeated after replacement of m , first by $2m$ and then by $3m$. The integrals and the derived Fourier coefficients are also shown in table 5. It will be seen that ζ_{3m} is much smaller than the two preceding terms, which have the same order of magnitude.

12. THE EQUATORIAL DISTRIBUTION OF TIDAL CONSTITUENT K_2

With the mean elevation ζ_0 and the three coefficients ζ_m , ζ_{2m} and ζ_{3m} it was possible to ascertain the amplitude and phase of K_2 at any point on the equator. The coefficient of the term in $\cos m\chi$ in the series for the constituent may be written $\zeta_m = (\zeta_{1,m} + i\zeta_{2,m}) e^{2i\omega t}$, thus the real part is $\zeta_{1,m} \cos 2\omega t - \zeta_{2,m} \sin 2\omega t$. The other coefficients may be treated in similar fashion and with $\zeta_0 = (\zeta_{1,0} + i\zeta_{2,0}) e^{2i\omega t}$, the Fourier series becomes

$$\begin{aligned}
 \zeta_{K_2} = & (\zeta_{1,0} + \zeta_{1,m} \cos m\chi + \zeta_{1,2m} \cos 2m\chi + \zeta_{1,3m} \cos 3m\chi + \dots) \cos 2\omega t \\
 & - (\zeta_{2,0} + \zeta_{2,m} \cos m\chi + \zeta_{2,2m} \cos 2m\chi + \zeta_{2,3m} \cos 3m\chi + \dots) \sin 2\omega t.
 \end{aligned}$$

The amplitude and the phase of the constituent were calculated on the coasts where $\chi = 0$ and $\chi = 56.6^\circ$. At first it was found that while there was fairly good agreement with the known equatorial values on the coast of Africa, the results for the coast at Sumatra showed some deviation. After revising the interpolated harmonic constants in the shallow-water regions where the uncertainty was greatest, and on recalculating all the coastal integrals, this divergence was almost eliminated and even better values were obtained for the African coast. On the equatorial coasts of Africa and Sumatra the harmonic constants are $H = 9.5$ cm, $g_1 = 217^\circ$ and $H = 3.0$ cm, $g_1 = 160^\circ$, respectively. Those obtained from the Fourier series are $H = 9.8$ cm, $g_1 = 220^\circ$ and $H = 2.8$ cm, $g_1 = 166^\circ$, respectively. The corrected coefficients, given in tables 4 and 5, were used to calculate the amplitude and phase at intervals of 2.5° between $\chi = 2.5^\circ$ and $\chi = 55^\circ$, and graphs showing H and g_1 are presented in figure 5. The prominent features of these graphs are the small amplitude and rapid change of phase between $\chi = 15^\circ$ and $\chi = 25^\circ$. This combination suggests the presence of an amphidromic region near the equator, especially when the coastal distribution of the constituent is examined. Other interesting features are the extensive region of virtually constant phase between $\chi = 25^\circ$ and $\chi = 40^\circ$, and the small amplitude but rapidly changing phase near the coast of Sumatra. In the latter the phase changes correspond very closely with similar changes on the east coast of Ceylon, where the amplitude is also of the same order of magnitude.

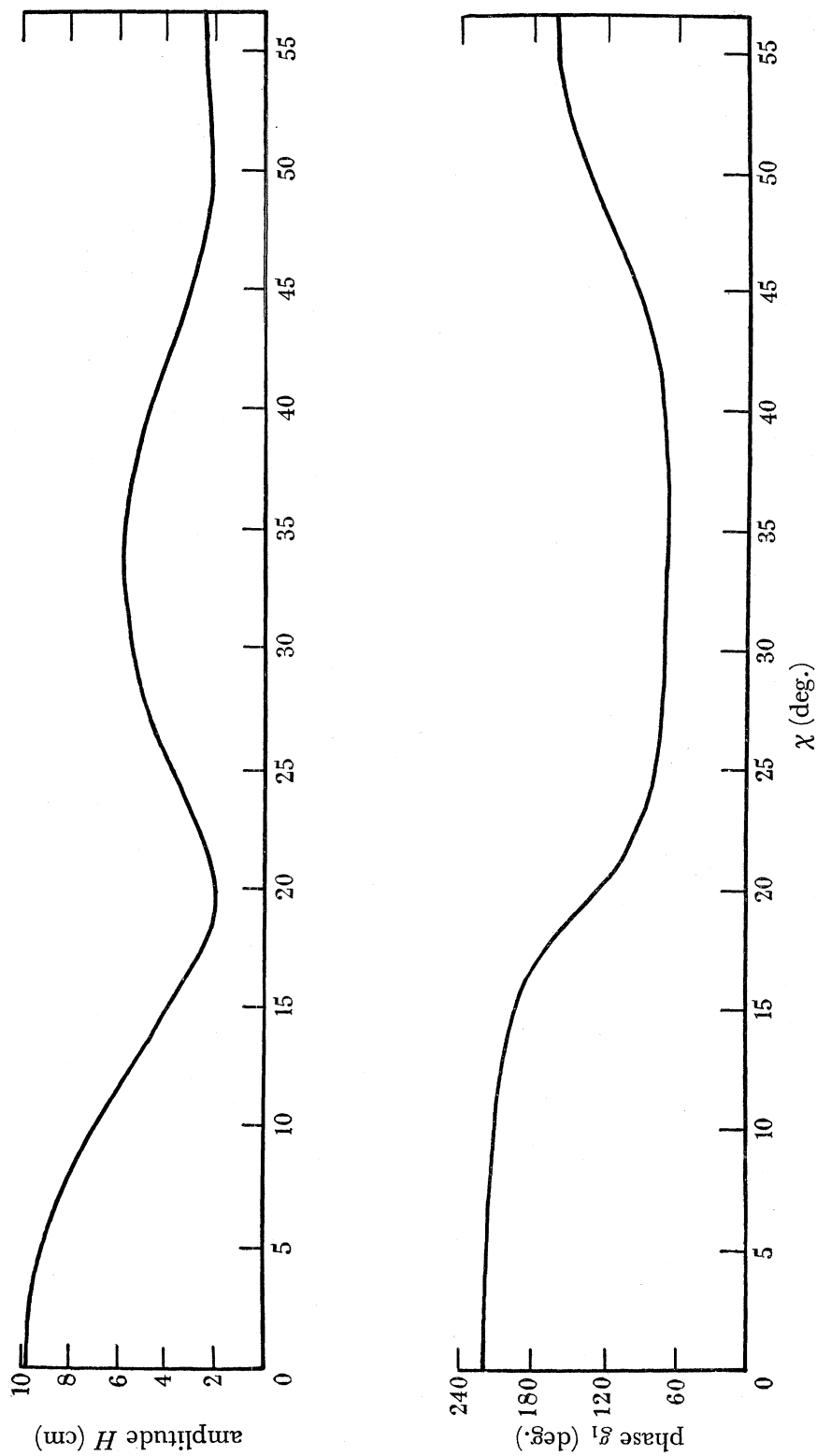


FIGURE 5. Variation of amplitude H and phase g_1 along the equator.

With the original coastal data and the deduced values along the equator a chart was drawn to show the co-tidal and co-range lines in the northern part of the Indian Ocean. The chart, figure 6, has much in common with the co-tidal charts for the semi-diurnal constituent M_2 given by Harris, Sterneck, Dietrich and Villain. The amphidromic point between African and India and the concentration of co-tidal lines between Ceylon and Sumatra are common to all five charts. In the earlier charts, however, no attempt was made to insert the co-range lines.

13. DISCUSSION OF THE RESULTS

The fundamental requirement of this method for calculation of tidal distribution is an accurate and complete knowledge of the constituent along the coastal boundaries. In this present application there are some regions where few harmonic constituents are as yet known; thus interpolation, with its attendant uncertainties, is required in places where there may actually be rapid changes in amplitude and phase. For an ocean of constant depth it is essential to adjust the harmonic constants in areas of shallow water. The necessity for this may be seen by considering the nature of the auxiliary functions, where values increase rapidly with latitude and also with increasing multiples of m . With large auxiliary functions, magnified coastal elevations would bias the values of the coastal integrals, those values on the northern shores of India providing an excellent example of this effect. In such circumstances the relatively small modifications to interpolated harmonic constants in these areas, producing a better fit for the distribution at the equatorial coastal points, are considered to be justified. Even without these adjustments, however, the major features of the final distribution were apparent.

An alternative procedure would be to use variable depth over the ocean, requiring different development of the auxiliary functions. In the present case it is felt that this would be of doubtful value until an appreciably greater quantity of tidal data becomes available.

In addition to the neglect of frictional forces, no allowance has been made for the yielding of the solid earth under tidal action. If the tidal elevations around the coastal boundary of the area were known with great accuracy it might be possible to deduce the yielding of the solid earth by using the equations of 'fit' at the ends of the bounding chord.

The equatorial distribution of K_2 provides supporting evidence for the phase relations embodied in the various co-tidal charts already discussed. In the present work, however, the variations have been deduced by dynamical methods using observational data, not from consideration of tidal oscillations in ocean basins or merely from interpolation of coastal values. Furthermore, an estimate of the amplitude of the K_2 constituent has now been given for any point on the equator.

The theorem has only been applied along the equator, but it could equally well be used for any other parallel of latitude. In doing so it would be necessary to compute a new series of auxiliary functions. Repetition of the procedure in a number of different latitudes would facilitate the constructions of comprehensive co-tidal and co-range charts. The extension of the method to other tidal constituents is now being considered, in particular to M_2 , where additional tidal data are available in the form of inferred harmonic constants given in the *Admiralty tide tables*, part II, 1938. This extension would produce more complex arithmetical processes in the work because angular speeds other than 2ω would make equations (15),

ALONG THE EQUATOR IN THE INDIAN OCEAN

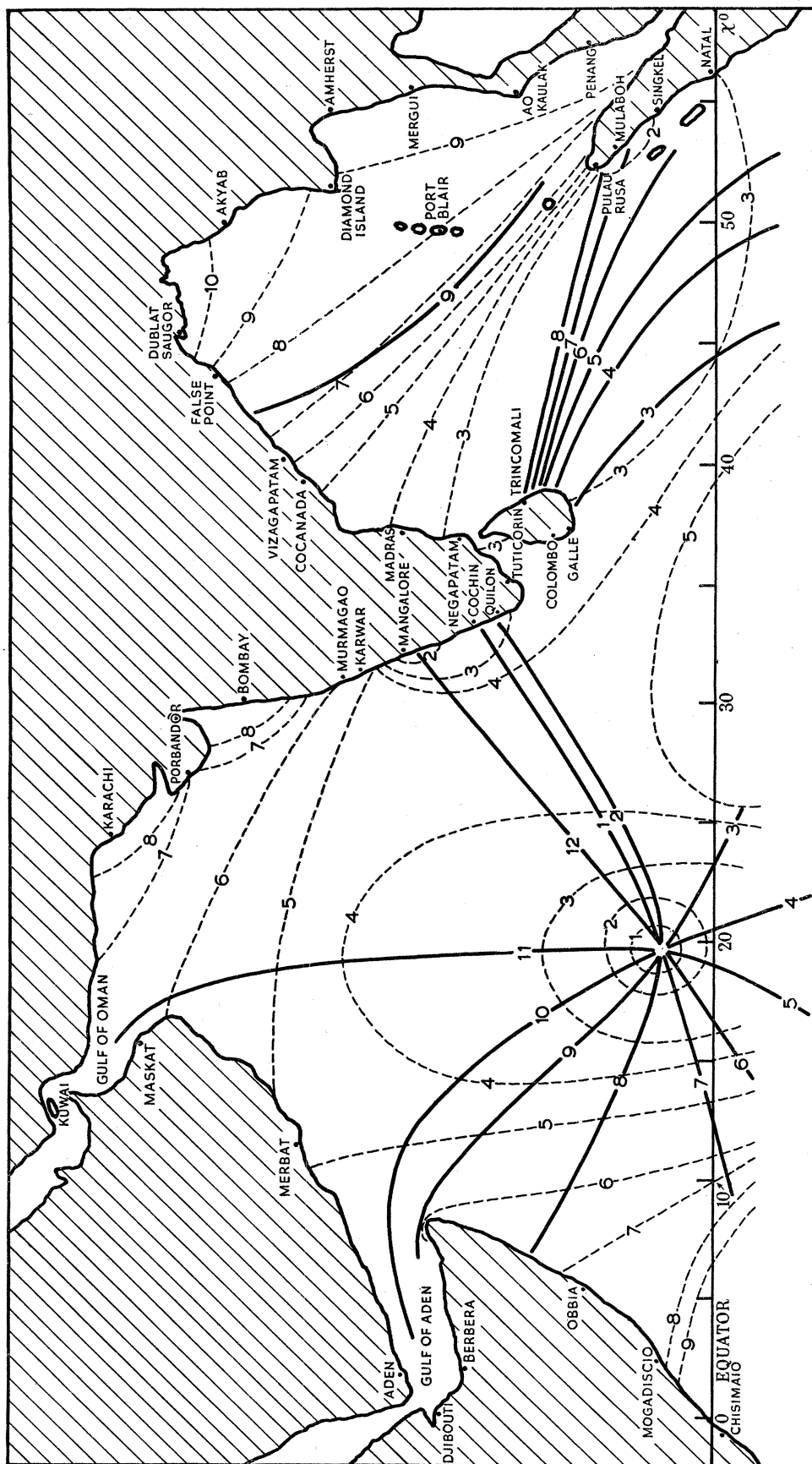


FIGURE 6. Co-tidal and co-range lines for constituent K_2 . The numbers on the full lines give the time of high water in hours which are one-twelfth of the period, the time origin being on the standard meridian where $\chi = 32^\circ$. The numbers on the broken lines give the amplitude H in cm.

(16), (24) and (25), and their subsequent development, more elaborate. It is also proposed to apply the theorem to the northern part of the Pacific, where the narrow Bering Straits constitute the only major water boundary. In this instance the ocean extends over a greater range of latitude, thus increasing the amount of computation when finding the auxiliary functions. The greater range of longitude, on the other hand, substantially reduces the value of m , so the arithmetical work may, in fact, prove to be less arduous.

It is a great pleasure to record my thanks to Professor J. Proudman, F.R.S., for his interest and encouragement in this work, which he initiated, and to Dr C. W. Jones for his advice on computational methods.

REFERENCES

- Defant, A. 1924 *Ann. Hydrogr.* **52**, 153, 177.
 Defant, A. 1932 *Wiss. Ergebn. dtsh. atlant. Exped. 'Meteor'*, **7** (1), 273.
 Dietrich, G. 1944 *Veröff. Inst. Meeresh. Univ. Berl.* A41.
 Doodson, A. T. 1928 *Mon. Not. R. Astr. Soc. Geophys. Suppl.* **1**, 541.
 Fox, L. & Goodwin, E. T. 1948 *Proc. Camb. Phil. Soc.* **45**, 373.
 Hansen, W. 1949 *Dtsch. hydrogr. Z.* **2**, 44.
 Harris, R. A. 1904 *Manual of tides*, pt. IVB. U.S.C.G.S. Washington, D.C.
 Proudman, J. 1925 *Phil. Mag.* **49**, 465.
 Proudman, J. 1944 *Mon. Not. R. Astr. Soc.* **104**, 244.
 Proudman, J. 1953 *Dynamical oceanography*, p. 230. London: Methuen.
 Sterneck, R. 1920 *S.B. Akad. Wiss. Wien*, 11a, **129**, 131.
 Villain, C. 1951 *Bull. Inform. C.O.E.C.* no. 9, 370.
 Whewell, W. 1833 *Phil. Trans.* p. 147.